Instabilities and solitons in systems with spatio-temporal dispersions and non paraxial approximations

Monisha Kumar, K. Nithyanandan, Houria Triki, K. Porsezian

Version of Record: https://www.sciencedirect.com/science/article/pii/S0030402619301342
Manuscript_59427d19370bac82ce686aba804f24ac

Instabilities and solitons in systems with spatio-temporal dispersions and non paraxial approximations

Monisha Kumar[a], K. Nithyanandan[b,c,*], Houria Triki[d], K.Porsezian[a]

[a] *Department of Physics,Pondicherry University, Puducherry, India 605014*
[b] *Laboratoire Interdisciplinaire Carnot de Bourgogne, UMR 6303 CNRS, Univ. Bourgogne Franche-Comté, 9 Av. A. Savary, B.P. 47870, 21078 Dijon Cedex, France.*
[c] *CNRS/Universite Joseph Fourier, Laboratoire Interdisciplinaire de Physique (LIPHY), 38402 Saint-Martin-d'Héres, Grenoble, France.*
[d] *Radiation Physics Laboratory, Department of Physics, Faculty of Sciences, Badji Mokhtar University, P.O. Box 12, 23000 Annaba, Algeria.*

Abstract

We consider the evolution of light beams in nonlinear Kerr media wherein the beam propagation is governed by the coupled non-paraxial (2+1) dimensional nonlinear Schrödinger equation. In the advent of system failing to obey the slowly varying envelope approximation, the usual paraxial approximation cannot be adopted. Our model equation could potentially serve as a governing model for nano-waveguides and on-chip silicon photonic devices. Using the trial solution method, we derive the different combinations of soliton solutions such as bright-bright, dark-dark, and bright-dark soliton and briefly discuss the characteristics of the soliton. Following the initial discussion on the soliton solution, we extend the study to investigate the modulational instability of the system of equations. We examine the role of the dispersion/diffraction in the instability spectra and demonstrate the different characteristics of the instability bands as a function of system parameters.

*Corresponding author
Email addresses: monisha.babykumar@gmail.com (Monisha Kumar), nithi.physics@gmail.com (K. Nithyanandan)

1. Introduction

The propagation of optical beam down the optical fiber is given by the celebrated nonlinear Schrödinger equation (NLSE). NLSE has been very successful in explaining the pulse/beam propagation through optical waveguides for more than three decades. However, the NLSE is tailor-made for optical pulse propagation in fiber like waveguide structure under some strict assumption. One of the important approximation is the so-called slowly varying envelope approximation (SVEA). The SVEA is able to provide an adequate description only if the optical beams are: (i) much broader than their carrier wavelength, (ii) of sufficiently low intensity and (iii) propagating along (or at near-negligible angles with respect to) the reference axis. These criteria define the paraxial approximation. If all the three conditions are not satisfied simultaneously, the beam is referred to as non-paraxial [1, 2]. Non-paraxiality is particularly prominent when there is miniaturization of devices. This show cases the importance of including the nonparaxial term into the NLSE while considering the light propagations in nano photonic waveguide devices.

Recently, there has been a lot of interest in the context of nonparaxial NLSE starting from Lax et al [3], especially on ultra narrow beams [4] where the condition (i) doesn't exist. Another area of research is the Helmholtz nonparaxial NLSE in the angular context where the condition (iii) is relaxed [5]. Blair has studied the scalar and vector nonlinear nonparaxial evolution equations for the propagation in two-dimensions. Exact and approximate solutions to these higher order evolution equation were also obtained which showed quasi-soliton behavior based on propagation and collision studies [6]. Numerical solutions to the nonparaxial NLS equation using the split-step Crank-Nicolson method were studied by Malakuti and Parilov [7] where they have shown that the nonparaxiality prevents the singularity formation and regularizes the solutions of NLSE. Temgoua and Kofane studied nonparaxial rogue waves in optical Kerr media [8], where they have shown that the nonparaxiality increases the intensity of rogue waves by increasing the length and reducing the peak width simultaneously. Also they noticed that the nonparaxial rogue waves are faster than the ones obtained from the standard NLS equation with the nonparaxiality moving the higher peak of rogue waves from the center to the periphery. At the same time, nonparaxiality causes the reduction in the interaction of the rogue waves. Chamorro-Posada et al [9] studied the nonparaxial spatial solitons which could be used in miniatur-

ized nonlinear photonic devices. They showed the exact nonparaxial soliton solution from which the paraxial soliton is recovered with appropriate limits. The soliton studies in the nonparaxial limit continues to earn more research interest in the recent times, owing to its fundamental and applied interest especially in the miniaturized photonic systems.

As an ubiquitous structures in nonlinear physics, the *soliton* appears to be a topic of intense research interest appearing in diverse fields such as nonlinear fiber optics [10, 11], matter waves in Bose-Einstein condensates [12], shallow water waves [13], molecular biology [14], ultrashort pulses in nonlinear optics [11, 15]. Temporal, spatial and spatiotemporal solitons find applications in almost all-optical routing, transparent beam interconnections, and the massive integration of optical operations in a fully three-dimensional environment. Two different types of envelope solitons, bright and dark, can propagate in nonlinear dispersive media. Compared with the bright soliton which is a pulse on a zero-intensity background, the dark soliton appears as an intensity dip in an infinitely extended constant background. Whenever linear effects (such as dispersion, diffraction or diffusion) are balanced exactly by nonlinearity (self-phase modulation, self-focusing or reaction-kinetic properties, respectively), robust self-trapped structures-solitons-can emerge as dominant modes of the system dynamics [1]. The exact soliton solution has been obtained for the dynamic equation of pulse propagation by a variety of methods such as Inverse scattering method [16, 17], Hirota bilinear transformation [18, 49], tanh method [20, 21], Sine-cosine method [22, 23], homogenous balance method [24, 25], exponential function method [26, 27], G'/G method [28, 29]. Out of many, trial solution method [30, 51, 32, 33, 52] is a direct and easier method of finding the exact solutions developed by Liu *et al*[35].

There are some recent studies as well. To mention a few, Liu *et.al* has studied different soliton solutions and their interactions and characteristic behaviors through the Hirota method [50]. Zhou *et.al* has studied the solitons in different media using the ansatz method/trial equation method and the inverse engineering methods [49]. Biswas *et.al* studied the soliton solutions through the modified simple equation method [51]. Also the soliton solutions in birefringent fibers with Kerr nonlinearity was studied by Ekici *et.al* through the exponential method [53], the soliton solution to the negative index materials with parabolic nonlinearity were studied by Mirza-

zadeh *et.al* [52]. Conservation laws for cubic-quartic optical solitons in media with Kerr and power law nonlinearities were studied by Belic *et.al* [54].

In the nonlinear system, the existence of solitons are very much related to the phenomenon of modulation instability (MI). MI is considered as a precursor to the soliton formation. MI is a phenomenon studied in many nonlinear systems, especially to nonlinear optics where there is an exponential growth of amplitude/phase perturbations of the input beam due to the interplay of diffraction/dispersion of the light beam with the nonlinearity of the system. This growing perturbations finally leads to the break down of the input beams into ultrashort pulses. Spatial and temporal MI have been vastly studied in many branches like, nonlinear fiber optics [36], Bose-Einstein Condensates [37], plasma physics [38], liquid crystals [39], plasmonics [40] and fluid dynamics [41]. However there has been only a few studies on spatio-temporal MI [42] and even fewer on nonparaxial NLSE [43]. To the best of our knowledge, there has not been any study on the MI of the coupled nonparaxial (2+1) NLSE.

Inspired by the recent work on the nonparaxial NLSE, in this paper, we investigate the propagation of optical pulse in the coupled nonparaxial (2+1) NLSE, where we derive the bright-bright, dark-dark and bright-dark soliton solutions. We further extend the study to investigate the MI and report the different characteristics of instability spectra under different settings. The paper is organized as follows: Section II presents the theoretical model and the propagation equations. Section III describes the soliton solutions, while MI analysis is reported in Section IV. Section V concludes the paper with summary of results.

2. Theoretical model

We study the general coupled nonparaxial (2+1) NLSE [44, 45] given in the dimensionless form as follows,

$$i\frac{\partial\Psi_1}{\partial z}+\kappa\frac{\partial^2\Psi_1}{\partial z^2}+s\frac{\partial^2\Psi_1}{\partial x^2}+\beta\frac{\partial^2\Psi_1}{\partial t^2}+\gamma_1|\Psi_1|^2\Psi_1+\gamma_2|\Psi_2|^2\Psi_1=0; \quad (1)$$

$$i\frac{\partial\Psi_2}{\partial z}+\kappa\frac{\partial^2\Psi_2}{\partial z^2}+s\frac{\partial^2\Psi_2}{\partial x^2}+\beta\frac{\partial^2\Psi_2}{\partial t^2}+\gamma_3|\Psi_2|^2\Psi_2+\gamma_4|\Psi_1|^2\Psi_2=0; \quad (2)$$

where,Ψ_1 and Ψ_2 are the space and time dependent amplitude of the propagating beam of light. z, x, t are the normalized spatial and temporal coordinates with z being the direction of propagation and x, the transverse direction. κ is the dimensionless coefficient of diffraction along the longitudinal direction z, s is the dimensionless coefficient of diffraction along the transverse direction. β decides the temporal dispersion to be anomalous or normal depending on β being positive or negative. $\gamma_1, \gamma_2, \gamma_3$ and γ_4 represents the coefficients of nonlinearity. Such that when $\gamma_2 = \gamma_3$ and $\gamma_1 = \gamma_4$ we have the modified Manakov NLSE model which simplifies to the normal Manakov model of NLSE when $\kappa = 0$. Similarly when $\gamma_1 = \gamma_3$ and $\gamma_2 = \gamma_4$ we have the normal nonparaxial coupled NLSE which simplifies to the usual coupled NLSE when κ becomes zero. In this case γ_1 is the coefficient of self phase modulation and γ_2 is the cross phase modulation. Here, we examine the problem of soliton propagation in the most general case, considering all coefficients of nonlinearities γ_i (with $i = 1, .., 4$) are unequal.

3. Soliton Solutions

There are different methods in practice to find the soliton solutions for a given equation. The choice of the methods are usually problem based and depends on the factors such as complexity, accuracy etc., Considering the complexity of the underlined problem we use the trial solution method as the choice, owing to its relative simplicity and accuracy. To start with, we rewrite Eq. (1) and (2) as,

$$i\frac{\partial \Psi_j}{\partial z} + \kappa\frac{\partial^2 \Psi_j}{\partial z^2} + s\frac{\partial^2 \Psi_j}{\partial x^2} + \beta\frac{\partial^2 \Psi_j}{\partial t^2} + \gamma_\sigma|\Psi_j|^2\Psi_j + \gamma_\xi|\Psi_{3-j}|^2\Psi_j = 0;\ j = 1, 2; \tag{3}$$

with σ=1, ξ=2 for j=1 and σ=3, ξ=4 for j=2.

We use the trial solution as

$$\Psi_j = f_j(U_j)e^{-i\phi_j(x,z,t)} \tag{4}$$

where $f_j(U_j)$ represents the shape of the pulse such that

$$U_j = b_j(t - v_j z - \eta_j x + \delta), \tag{5}$$

b_j represents the inverse width of soliton v_j and η_j represents the velocity of the soliton and the phase part is given by

$$\phi_j(z, x, t) = k_j z + m_j x - \omega_j t + \delta_0 \tag{6}$$

where j=1, 2. k_j and m_j represents the soliton wave numbers. ω_j represents the soliton frequency and δ_0 denotes the phase constant. Substituting Eq. (4) into Eq. (3) and separating the real and imaginary parts gives us the following equations.

$$(k_j - \kappa k_j^2 - s m_j^2 - \beta\omega_j^2 + \gamma_\sigma f_j(U_j)^2 + \gamma_\xi f_{3-j}(U_j)^2) f_j(U_j) + (b_j^2\beta + b_j^2 s\eta_j^2 + b_j^2 v_j^2\kappa) f_j''(U_j) = 0; \tag{7}$$

$$b_j(v_j - 2v_j\kappa k_j - 2s\eta_j m_j - 2\beta\omega_j) f_j'(U_j) = 0; \tag{8}$$

with j=1, 2, where $f_j'(U_j)$ and $f_j''(U_j)$ denotes df_j/dU_j and d^2f_j/dU_j^2, respectively. Since $f_j'(U_j)$ and b_j are non zero, simplifying (8) gives the velocity of solitons as

$$v_j = \frac{2(s\eta_j m_j + \beta\omega_j)}{1 - 2\kappa k_j};\ j = 1, 2; \tag{9}$$

3.1. Bright-Bright Soliton Solutions

Considering the bright soliton solutions to the above equations as

$$f_j(U_j) = A_j\ sech(U_j);\ j = 1, 2; \tag{10}$$

where A_j represents the soliton amplitude. Substituting Eq. (10) into Eq. (7), simplifying and separating the coefficients yields us the following equations:
(i)Separating the coefficients of $sech^3$ term gives us,

$$(-2b_j^2(\beta + s\eta_j^2 + v_j^2\kappa) + |A_j|^2\gamma_\sigma + |A_{3-j}|^2\gamma_\xi)A_j = 0;\ j = 1, 2; \tag{11}$$

(ii)Further, separating the coefficients of sech term yields us,

$$(b_j^2(\beta + s\eta_j^2 + v_j^2\kappa) + k_j(1 - \kappa k_j) - s m_j^2 - \beta\omega_j^2)A_j = 0;\ j = 1, 2; \tag{12}$$

Simplifying Eq. (12) gives us the expression for soliton width inverse b_j as

$$b_j = \pm\sqrt{\frac{-k_j + \kappa k_j^2 + s m_j^2 + \beta\omega_j^2}{\beta + s\eta_j^2 + v_j^2\kappa}};\ j = 1, 2; \tag{13}$$

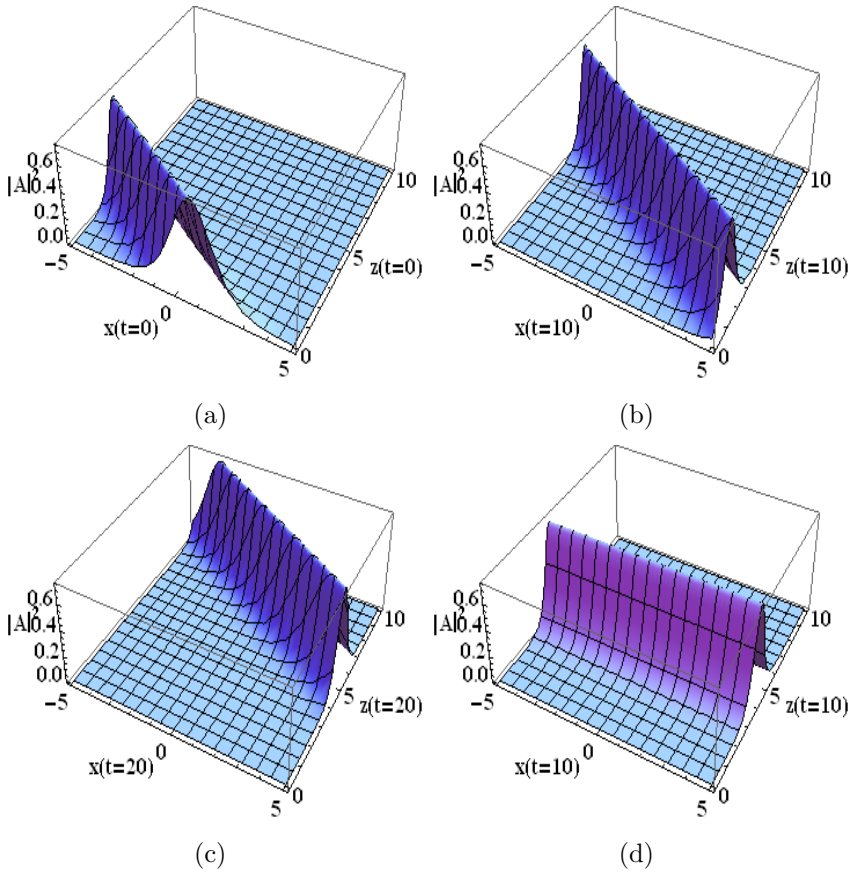

Figure 1: (Color online)(a) The evolution of bright soliton solution Ψ_1 for different values of time like (a) t = 0,(b)t = 10 (c)t = 20. (d) shows the soliton solution when, t = 10 and $\eta = 0$.

Similarly Eq. (11) gives us the expression for the soliton amplitudes. When j=1 we have

$$A_1 = \pm\sqrt{\frac{2b_1^2\beta + 2b_1^2 s\eta_1^2 + 2b_1^2 v_1^2\kappa - A_2^2\gamma_2}{\gamma_1}}; \tag{14}$$

and when j=2 we have

$$A_1 = \pm\sqrt{\frac{2b_2^2\beta + 2b_2^2 s\eta_2^2 + 2b_2^2 v_2^2\kappa - A_2^2\gamma_3}{\gamma_4}}; \tag{15}$$

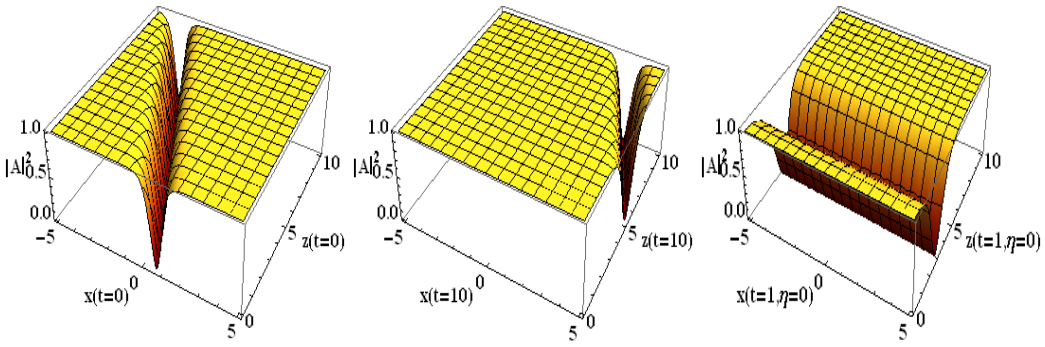

(a) (b) (c)

Figure 2: (Color online) The evolution of (2+1) spatio-temporal dark soliton solution ψ_1 for different time (a) t = 0, (b) t = 10, (c) t = 1 and the transverse - velocity $\eta = 0$.

Since Eq. (14) and Eq. (15) represents the amplitude of the same soliton, the two equations must be equal, which implies that if $b_1 = b_2$, value of A_1 can't be different. Thus from Eq. (14) and Eq. (15) we conclude that, γ_2=γ_3 and γ_1=γ_4. Hence we obtain the amplitude of the copropagating solitons as,

$$A_2 = \pm\sqrt{\frac{2b_2^2\beta + 2b_2^2 s\eta_2^2 + 2b_2^2 v_2^2\kappa - A_1^2\gamma_4}{\gamma_3}}; \tag{16}$$

As A_1, A_2, $1/b_j$ represents the soliton amplitudes and inverse pulse widths respectively, these parameters should be real which implies that $(\beta + s\eta_j^2 + v_j^2\kappa) \neq 0$ also $(\kappa\ k_j^2 + s\ m_j^2 + \beta\omega_j^2) > |k_j|$ for $(\beta + s\eta_j^2 + v_j^2\kappa) > 0$ and $(\kappa\ k_j^2 + s\ m_j^2 + \beta\omega_j^2) < |k_j|$ for $(\beta + s\eta_j^2 + v_j^2\kappa) < 0$. From Eq. (14), we find the essential condition for the existence of soliton solution is $2b_j^2(\beta + s\eta_j^2 + v_j^2\kappa) > A_2^2\gamma_2$ for $\gamma_1 > 0$ and $2b_j^2(\beta + s\eta_j^2 + v_j^2\kappa) < A_2^2\gamma_2$ for $\gamma_1 < 0$. Finally the bright soliton solution is given by

$$\Psi_j = \frac{\sqrt{(\beta + s\eta_j^2 + v_j^2\kappa)2b_j^2 - A_2^2\gamma_2}}{\sqrt{\gamma_1}} sech \frac{\sqrt{-k_j + \kappa k_j^2 + s m_j^2 + \beta\omega_j^2}}{\sqrt{\beta + s\eta_j^2 + v_j^2\kappa}}$$
$$(t - |v_j|z - \eta_j x + \delta)e^{-i(k_j z + m_j x - \omega_j t + \delta_0)};\ j = 1, 2; \tag{17}$$

If we assume, v_1=v_2, η_1=η_2=η, b_1=b_2 and k_1=k_2, then from Eq (9) the parameters ω_1 and ω_2 are related by

$$\omega_2 = \frac{s\eta}{\beta}(m_1 - m_2) + \omega_1 \tag{18}$$

and from Eq. (13) the parameters m_1 and m_2 are related by,

$$m_2 = \frac{2\omega_1\eta\beta + (s\eta^2 - \beta)m_1}{s\eta^2 + \beta} \tag{19}$$

Now we assume the following values for the system parameters $\kappa = 0.2$, s=0.2, $\beta = 0.2$ and the soliton parameters as $k_1 = k_2$=1, $m_1 = m_2 = 1$, $\omega_1 = \omega_2$=2.5 and η=1.5. So that from Eq. (9) we get the velocity of solitons as $v_1 = v_2 = 2.67$. Substituting this value of v_j into Eq. (13) along with other parameter values gives us the value of b_j as 0.6. Substituting the value b_j and v_j along with other parameter values into equations from (14) to (16) gives us the value of A_1=0.86, A_2=0.86.

Fig.1 shows the evolution of (2+1) spatio-temporal bright soliton solution ψ_1 for different values of time. The parameter values are the same as the one obtained above. Also we assume $\delta_0 = 1$ and $\delta = 1$. Fig 1(d) shows the same soliton solution when the velocity along transverse direction, η_j is made zero.

3.2. Dark-Dark Soliton Solutions

In order to find the dark soliton solution, we consider the solution of the form,

$$f_j = A_j \; tanh \; U_j; \; j = 1, 2; \tag{20}$$

Substituting Eq. (20) into Eq. (7), simplifying and separating the coefficients following the same procedure above, yields us the parameters of dark soliton as,

$$b_j = \pm\frac{\sqrt{k_j - \kappa k_j^2 - s m_j^2 - \beta\omega_j^2}}{\sqrt{2}\sqrt{\beta + s\eta_j^2 + v_j^2\kappa}}; \; j = 1, 2; \tag{21}$$

$$A_1 = \pm\frac{\sqrt{-(2b_1^2\beta + 2b_1^2 s\eta_1^2 + 2b_1^2 v_1^2\kappa + A_2^2\gamma_2)}}{\sqrt{\gamma_1}} \tag{22}$$

$$A_2 = \pm\frac{\sqrt{-(2b_1^2\beta + 2b_1^2 s\eta_1^2 + 2b_1^2 v_1^2\kappa + A_1^2\gamma_1)}}{\sqrt{\gamma_2}} \tag{23}$$

$$A_1 = \pm\frac{\sqrt{-(2b_2^2\beta + 2b_2^2 s\eta_2^2 + 2b_2^2 v_2^2\kappa + A_2^2\gamma_3)}}{\sqrt{\gamma_4}} \tag{24}$$

$$A_2 = \pm\frac{\sqrt{-(2b_1^2\beta + 2b_1^2 s\eta_1^2 + 2b_1^2 v_1^2\kappa + A_1^2\gamma_4)}}{\sqrt{\gamma_3}} \tag{25}$$

Analogous to the previous sections, Eq. (22) and (24), (23) and (25) leads us to the conclusion that, γ_1=γ_4 and γ_2=γ_3. Since A_1, A_2, $1/b_j$ are the amplitudes and width of the solitons, these parameters must be real, which gives the following constraints for the existence of the soliton solution.
For the dark soliton solution to exist, γ_1 and γ_2 cannot be simultaneously greater than zero. If γ_1 and γ_2 is negative, then the condition $|2b_j^2(\beta + s\eta_j^2 + v_j^2\kappa)| > |A_{2(1)}^2\gamma_{2(1)}|$ should be satisfied for the existence of dark soliton solution. If γ_1 is positive and γ_2 is negative, then $|2b_j^2(\beta+s\eta_j^2+v_j^2\kappa)| < |A_2^2\gamma_2|$ should be satisfied for the dark soliton solution to exist and if γ_1 is negative and γ_2 is positive, then $|2b_j^2(\beta + s\eta_j^2 + v_j^2\kappa)| < |A_1^2\gamma_1|$ is the condition to be satisfied. Similarly equation (27) shows that the dark soliton solution can exist if $(\beta + s\eta_j^2 + v_j^2\kappa) > 0$ for $|\mathrm{k}_j| > |\kappa\ \mathrm{k}_j^2 + \mathrm{s}\ \mathrm{m}_j^2 + \beta\omega_j^2|$ and if $|\mathrm{k}_j| < |\kappa\ \mathrm{k}_j^2 + \mathrm{s}\ \mathrm{m}_j^2 + \beta\omega_j^2|$ for $(\beta+\mathrm{s}\eta_j^2 + v_j^2\kappa) < 0$ which is same as the bright solitons.

Finally the dark soliton solution in its full form is,

$$\Psi_j = \pm\frac{\sqrt{-2b_j^2\beta - 2b_j^2 s\eta_j^2 - 2b_j^2 v_j^2\kappa - B^2\gamma_2}}{\sqrt{\gamma_1}} tanh\frac{\sqrt{k_j - \kappa k_j^2 - s m_j^2 - \beta\omega_j^2)}}{\sqrt{2(\beta + s\eta^2 + v_j^2\kappa)}}$$
$$(t - |v_j|z - \eta x + \delta)e^{-i(k_j z + m_j x - \omega_j t + \delta_0)};\ j = 1, 2; \tag{26}$$

where v_j, ω_j and m_j are the same as given by Eq. (9), (18) and (19) respectively, when the following conditions b_1=b_2, v_1=v_2 = v, η_1=η_2=η and k_1=k_2 are satisfied. We assume the following parameter values $k_1 = k_2 = m_1 = m_2 = 1$, $\omega_1 = \omega_2 = 2.5$, $\eta = 1.5$, β = -0.2, $\kappa = 0.2$, s = 0.2, $\gamma_1 = \gamma_2$ = -1. Substituting these values into equation (9) gives us the value of longitudinal velocity $v = 0.66$ which further gives the value of b_j from (21) as 1.69. Similarly (22) and (23) gives the value of $A_1 = 0.92$ with the assumption $A_2 = 1$. In Fig.2 we have the evolution of (2+1) spatio-temporal dark soliton solution ψ_1 for different values of time (a) t = 0, (b) t = 10, (c) t = 1 and the transverse velocity $\eta = 0$.

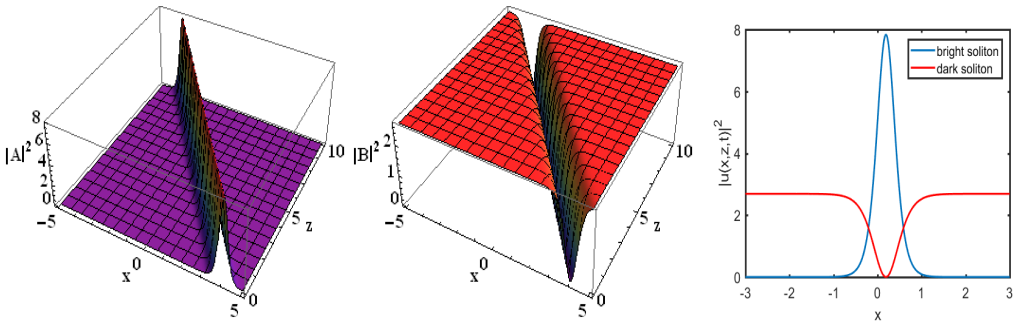

(a) (b) (c)

Figure 3: (Color online) The evolution of (2+1) spatio-temporal bright-dark soliton solutions (a) $|\psi_1|^2$ (b) $|\psi_2|^2$ for t=5. (c)Shows the corresponding 2D plot for the same with t=5 and z

3.3. Bright-Dark Soliton Solutions

We consider the bright-dark soliton solutions of the following form

$$\Psi_1 = A\ sech(U_1)e^{i\Phi_1}; \tag{27}$$

$$\Psi_2 = B\ tanh(U_2)e^{i\Phi_2} \tag{28}$$

Substituting Eq. (27) and (28) into Eq. (1) and (2), and following the procedure same as the previous section, we obtain the soliton parameters as:

$$b_1 = \pm\sqrt{\frac{k_1 + \kappa k_1^2 + sm_1^2 + \beta\omega_1^2 - B^2\gamma_2}{\beta + s\eta_1^2 + v_1^2\kappa}} \tag{29}$$

$$A = \pm\sqrt{\frac{2b_1^2(\beta + s\eta_1^2 + v_1^2\kappa) + B^2\gamma_2}{\gamma_1}} \tag{30}$$

$$v_1 = \frac{-2(s\eta_1 m_1 + \beta\omega_1)}{1 + 2\kappa k_1} \tag{31}$$

$$v_2 = -\frac{2(s\eta_2 m_2 + \beta\omega_2)}{1 - 2\kappa k_2} \tag{32}$$

$$B = \pm\sqrt{\frac{-2b_2^2(\beta + s\eta_2^2 + v_2^2\kappa) + A^2\gamma_4}{\gamma_3}} \tag{33}$$

$$b_2 = \pm\sqrt{\frac{-k_2 - \kappa k_2^2 - sm_2^2 - \beta\omega_2^2 + A^2\gamma_4}{2(\beta + s\eta_2^2 + v_2^2\kappa)}} \tag{34}$$

Further equation (29) in (30) helps in deducing the expressions of bright soliton amplitudes to,

$$A = \pm\frac{\sqrt{2(k_1 + \kappa k_1^2 + sm_1^2 + \beta\omega_1^2) - B^2\gamma_2}}{\sqrt{\gamma_1}}; \tag{35}$$

Similarly Eq. (34) in (33) yields us the amplitude of dark soliton B to,

$$B = \pm\frac{\sqrt{(k_2 + \kappa k_2^2 + sm_2^2 + \beta\omega_2^2)}}{\sqrt{\gamma_3}}; \tag{36}$$

Thus the final form of bright-dark soliton solutions is,

$$\Psi_1 = \pm\frac{\sqrt{2b_1^2(\beta + s\eta_1^2 + v_1^2\kappa) + B^2\gamma_2}}{\sqrt{\gamma_1}} sech$$
$$\frac{\sqrt{k_1 + \kappa k_1^2 + sm_1^2 + \beta\omega_1^2 - B^2\gamma_2)}}{\sqrt{\beta + s\eta_1^2 + v_1^2\kappa}}(t - |v_1|z - \eta_1 x + \delta)$$
$$e^{i(k_1 z + m_1 x - \omega_1 t + \delta_0)}; \tag{37}$$

$$\Psi_2 = \pm\frac{\sqrt{-2b_2^2(\beta + s\eta_2^2 + v_2^2\kappa + A^2\gamma_4}}{\sqrt{\gamma_3}} tanh$$
$$\frac{\sqrt{-(k_2 + \kappa k_2^2 + sm_2^2 + \beta\omega_2^2) + A^2\gamma_4}}{\sqrt{2(\beta + s\eta_2^2 + v_2^2\kappa)}}(t - |v_2|z - \eta x + \delta)$$
$$e^{i(k_2 z + m_2 x - \omega_2 t + \delta_0)}; \tag{38}$$

Fig.3 shows the bright-dark solitons for the parameter values $k_1 = k_2 = m_1 = m_2 = 1$, $\beta = \kappa$ =s=0.2, $\eta_1 = \eta_2 = \eta = 1.5$, $v_1 = v_2 = 1.143$, A=2.8, $\omega_1 = \omega_2$=2.5, B=1.62, $\gamma_1 = \gamma_3 = \gamma_4$=1, γ_2=-1, b_1=2.41, b_2=1.7, t=5.

4. Linear Stability Analysis

Most nonlinear systems exhibit instability against perturbation which inturn leads to the modulation of their steady states by the interplay between their nonlinearity and dispersion/diffraction. In order to study the MI for the above equation, we use the standard linear stability analysis. Here we consider the steady state solution to the above mentioned system which is given by,

$$\psi_1(x,z,t) = \sqrt{P_0}e^{i\Phi_1 z}; \tag{39}$$

$$\psi_2(x,z,t) = \sqrt{P_0}e^{i\Phi_2 z}; \tag{40}$$

where $\omega_1 = \frac{-1\pm\sqrt{1+4\kappa P_0(\gamma_1+\gamma_2)}}{2\kappa}$ and $\omega_2 = \frac{-1\pm\sqrt{1+4\kappa P_0(\gamma_3+\gamma_4)}}{2\kappa}$ are the nonlinearity induced phase shifts. In order to study the stability of the system, we add a small perturbation into the system so that the perturbed solution is given by,

$$\psi_1(x,z,t) = (\sqrt{P_0} + a(x,z,t))e^{i\Phi_1 z}; \tag{41}$$

$$\psi_2(x,z,t) = (\sqrt{P_0} + b(x,z,t))e^{i\Phi_2 z}; \tag{42}$$

where the complex fields $|a(x,z,t)| \ll \sqrt{P_0}$ and $|b(x,z,t)| \ll \sqrt{P_0}$. Substituting Eqs. (41) and (42) into Eqs. (1) and (2) and collecting terms of $a(x,z,t)$ and $b(x,z,t)$, we obtain the coupled linearized equations of the perturbed fields,

$$\begin{aligned} &P_0(\gamma_1(a(x,z,t)+a^*(x,z,t)) + \gamma_2(b(x,z,t)+b^*(x,z,t))) \\ &+\beta\frac{\partial a^2(x,z,t)}{\partial^2 t} - i\sqrt{1+4\kappa P_0(\gamma_1+\gamma_2)}\frac{\partial a(x,z,t)}{\partial z} + \\ &\kappa\frac{\partial a^2(x,z,t)}{\partial^2 z} + s\frac{\partial a^2(x,z,t)}{\partial^2 x} = 0; \end{aligned} \tag{43}$$

$$\begin{aligned} &P_0(\gamma_4(a(x,z,t)+a^*(x,z,t)) + \gamma_3(b(x,z,t)+b^*(x,z,t))) \\ &+\beta\frac{\partial b^2(x,z,t)}{\partial^2 t} - i\sqrt{1+4\kappa P_0(\gamma_3+\gamma_4)}\frac{\partial b(x,z,t)}{\partial z} \\ &+\kappa\frac{\partial b^2(x,z,t)}{\partial^2 z} + s\frac{\partial b^2(x,z,t)}{\partial^2 x} = 0 \end{aligned} \tag{44}$$

Here, $a^*(x,z,t)$ and $b^*(x,z,t)$ are the complex conjugate of the perturbed fields. Now we assume the following ansatz for the perturbations $a(x,z,t)$ and $b(x,z,t)$,

$$a(x,z,t) = F_1 e^{i(\mu x+\lambda z-\Omega t)} + G_1 e^{-i(\mu x+\lambda z-\Omega t)} \tag{45}$$

$$b(x,z,t) = F_2 e^{i(\mu x+\lambda z-\Omega t)} + G_2 e^{-i(\mu x+\lambda z-\Omega t)} \tag{46}$$

with F_1, G_1, F_2, G_2 forming the amplitudes of the perturbation which are real. μ and λ are the wave vectors of the perturbation in the transverse and longitudinal direction of propagation, respectively. Ω is the frequency of perturbation. Substituting Eq. (45) and (46) into Eq. (43) and (44) we obtain the following stability matrix

$$\begin{pmatrix} \mathbf{m_{11}} & \mathbf{m_{12}} & \mathbf{m_{13}} & \mathbf{m_{14}} \\ \mathbf{m_{21}} & \mathbf{m_{22}} & \mathbf{m_{23}} & \mathbf{m_{24}} \\ \mathbf{m_{31}} & \mathbf{m_{32}} & \mathbf{m_{33}} & \mathbf{m_{34}} \\ \mathbf{m_{41}} & \mathbf{m_{42}} & \mathbf{m_{43}} & \mathbf{m_{44}} \end{pmatrix}$$

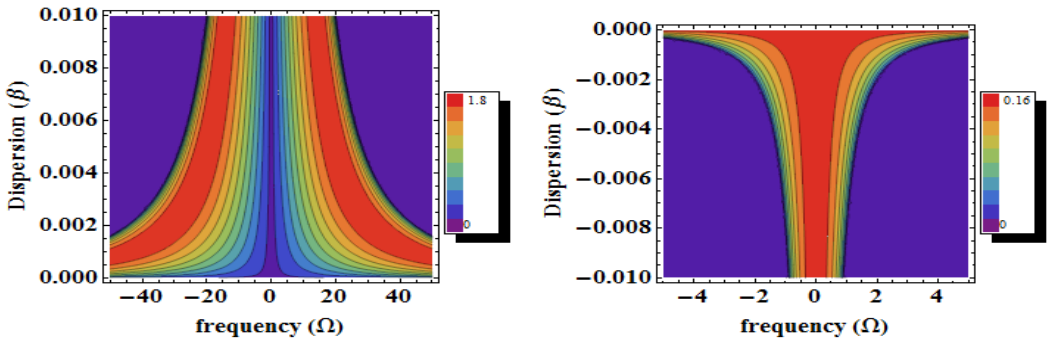

(a) (b)

Figure 4: (Color online) The contour plots of MI spectra (a) in the anomalous dispersion regime, (b) the normal dispersion regime, with other parameters as $\kappa = 0.005$ and s=0.002, $P_0 = 1, \gamma_1 = 1, \gamma_2 = 1, \mu = 2$.

where $\mathbf{m_{11}} = -\kappa\lambda^2 - s\mu^2 - \beta\Omega^2 + \mathbf{m_{12}} + \lambda\sqrt{1+4\kappa P_0(\gamma_1+\gamma_2)}$;$\mathbf{m_{12}}$=$\mathbf{m_{21}}$= $P_0\gamma_1$; $\mathbf{m_{13}}$=$\mathbf{m_{23}}$=$\mathbf{m_{14}}$=$\mathbf{m_{24}}$=$P_0\gamma_2$; $\mathbf{m_{34}}$=$\mathbf{m_{43}}$=$P_0\gamma_3$; $\mathbf{m_{31}}$=$\mathbf{m_{32}}$=$\mathbf{m_{41}}$=$\mathbf{m_{42}}$ = $P_0\gamma_4$; $\mathbf{m_{22}} = -\kappa\lambda^2 - s\mu^2 - \beta\Omega^2 + \mathbf{m_{12}} - \lambda\sqrt{1+4\kappa P_0(\gamma_1+\gamma_2)}$; $\mathbf{m_{33}} = -\kappa\lambda^2 - s\mu^2 - \beta\Omega^2 + \mathbf{m_{34}} + \lambda\sqrt{1+4\kappa P_0(\gamma_3+\gamma_4)}$; $\mathbf{m_{44}} = -\kappa\lambda^2 - s\mu^2 - \beta\Omega^2 + \mathbf{m_{34}} - \lambda\sqrt{1+4\kappa P_0(\gamma_3+\gamma_4)}$; From the above matrix, using the assumption γ_1=γ_4 and γ_2=γ_3 we arrive at the dispersion relation for λ given by,

$$\lambda = \frac{1}{\sqrt{2\kappa^2}}\sqrt{-X_1 + \sqrt{X_2})} \tag{47}$$

where X_1=$(-1 + 2s\kappa\mu^2 + 2\beta\kappa\Omega^2 - 6\kappa P_0\gamma$ and X_2=$1 - 4\kappa(s\mu^2 + \beta\Omega^2) + 4\kappa P_0\gamma(3 - 4\kappa(s\mu^2 + \beta\Omega^2) + 9\kappa P_0\gamma)$ where $\gamma = \gamma_1 + \gamma_2$. MI occurs when the wave vector λ has a nonzero imaginary part leading to an exponential growth of the perturbed amplitudes. The growth rate of the MI gain is defined as

$$G(\Omega) = 2|Im\ \lambda| \tag{48}$$

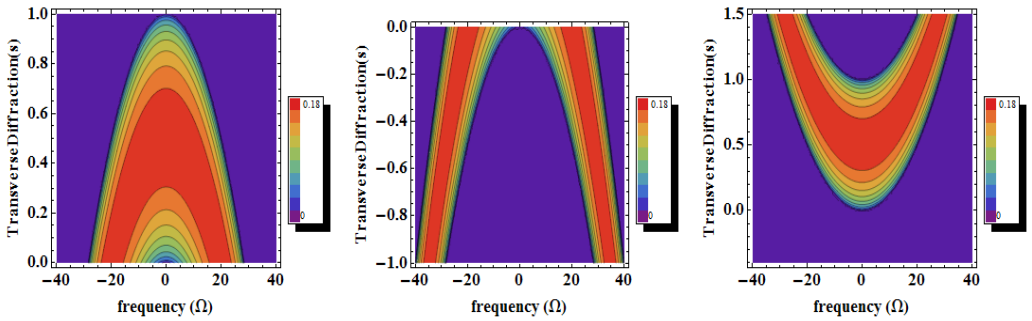

(a) (b) (c)

Figure 5: (Color online)(a) The contour plots of MI spectra with the transverse diffraction parameter s in different dispersion regimes. (a) s being positive in the anomalous dispersion region with $\beta = 0.005$ (b) s being negative in the anomalous dispersion region with $\beta = 0.005$ (c) s being positive in the normal dispersion region with $\beta = -0.005$. The other parameters are taken as $P_0 = 1, \gamma_1 = 1, \gamma_2 = 1, \kappa = 0.005, \mu = 2$.

5. Modulational Instability

Using Eq. (48), in what follows, we briefly analyze the MI for a coupled system of nonparaxial NLSE for the first time to the best of our knowledge. Particularly, our emphasize is on the effect of diffractions and dispersion in the instability spectra.

5.1. The effect of dispersion

For studying the effect of dispersion on MI, we varied β from -10^{-5} to -10^{-2} and 10^{-5} to 10^{-2}. We observe that, there is no change in maximum gain value, but the MI bandwidth (Ω_{BW}) changes drastically as seen in the

Table 1: **: MI behaviors for different parameters**

β	κ	s	$MI\ Gain\ (\Omega)$
$-ve$	$+ve$	$+ve$	$Only\ G(0)\ peak$
$-ve$	$-ve$	$+ve$	$Only\ G(0)\ peak$
$-ve$	$+ve$	$-ve$	$No\ MI\ gain$
$-ve$	$-ve$	$-ve$	$No\ MI\ gain$

contour plots of fig 4.

From fig. (4(a)), we note that for the anomalous dispersion ($\beta > 0$), the Ω_{BW} drastically reduces as β increases for a positive value of transverse diffraction, s. But when s is negative, the two sidebands of MI is separated from the central frequency and the separation of sidebands is more for a lower value of β. Also, we notice that the sign of κ hardly influence the instability spectra in this parametric regime. In the normal dispersion ($\beta < 0$) regime, from fig (4(b)) we note that there is no MI, but a single peak around the central frequency which implies amplification of the wave at the central frequency or the pump frequency and not the generation of sidebands. We note that the maximum gain value is lower for normal dispersion than the anomalous dispersion case. Here also we note that the bandwidth reduces as the value of $|\beta|$ increases. Table 1 shows the MI behavior of the system for different parameter values, which shows that in the normal dispersion regime when the system has a negative diffraction there is no gain in the system but the system shows MI gain for the same in the anomalous dispersion region.

5.2. The effect of transverse diffraction

To study the effect of transverse diffraction 's' on MI, we varied the value of s in the range of 0 to -0.6 as shown in fig (5). It is evident from the fig (5), the maximum gain of MI remain unchanged, while the optimum frequency corresponding to maximum gain shift to higher frequency side as $|s|$ increases. As in the previous case, the MI bandwidth reduces as $|\beta|$ increases. For the parameter of our choice, we noted that there is no MI for normal dispersion (β -ve) for s being -ve and κ is not deterministic to the origin of MI. In the regime of anomalous dispersion, for any positive values of transverse diffraction, the MI bandwidth decreases with increase in the s, while G_{max} remains constant. Interestingly, unlike the previous cases, the MI gain register a non-zero value for $\Omega = 0$, whose gain increases with increase in the strength of s. But for

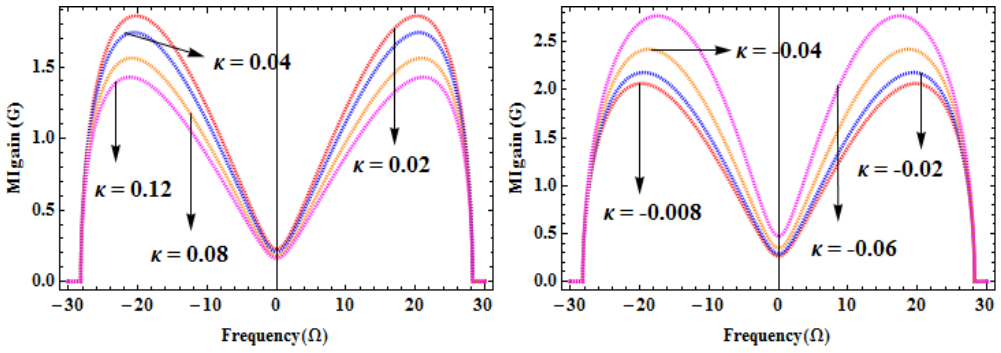

Figure 6: (Color online) The MI gain spectra for (a) different values of positive longitudinal diffraction κ and (b) for different values of negative longitudinal diffraction κ with other parameters as $P_0 = 1$, $\beta = 0.005$, $\gamma_1 = 1$, $\gamma_2 = 1$, s = 0.004.

the case of positive diffraction in the normal dispersion region, we notice that for low values of s only a single frequency around the central frequency is observed, which develops into a pair of sidebands on the either side of the central frequency for larger values of s. Another interesting point is that the MI is still possible in the anomalous dispersion (β +ve) region even if the transverse diffraction is absent.

5.3. The effect of longitudinal diffraction

Here we study the effect of longitudinal diffraction on MI, we keep the system to be in the anomalous dispersion regime with the transverse diffraction as positive. Fig 6(a) shows the behaivour of MI spectra for positive values of longitudinal diffractions which shows that G_{max} decreases with an increase in $|\kappa|$. But the zero frequency gain (G(0)) and Ω_{BW} remains unaffected. At the same time fig. 6(b) shows that the reverse happens when κ is negative i.e., G_{max} increases with increase in $|\kappa|$. Fig. 6(b) shows the instability spectra for negative values of κ, unlike the previous case the G_{max} increases with increase in κ. This shows that the effect of the sign of diffraction is absolutely crucial in determining the nature of the spectra.

6. Conclusion

In summary, we have modeled and studied the coupled non-paraxial (2+1) dimensional nonlinear Schrödinger equation without taking into account the famous slowly varying envelope approximation. To explore the propagation features of the proposed model in the waveguide structure, we have derived the soliton solutions under different settings using the trial solution method. For a comprehensive understanding of the underlined problem different combinations of the soliton solutions for instance, bright-bright, dark-dark, and bright-dark soliton have been derived in the non-paraxial limit. Following that, we have studied the modulational instability in the system of equations using linear stability analysis. An explicit dispersion relation has been derived and MI analysis is performed under different parametric conditions, with an emphasize on the role of the dispersion and diffraction parameter in the instability spectra. We have reported that the sign of the disperion/diffraction parameter is fundamental to the origin of MI and the magnitude of which determines the strength of gain and bandwidth of MI.

To conclude, our detailed theoretical analysis reveals the NLSE qualitatively differs in the non-paraxial limit. Particularly, in the miniaturized system such as nano-waveguide, the paraxial approximation used in the NLSE is less favorable and therefore one have to modify the standard NLSE without SVEA as discussed in the present context. With the advancement of on-chip silicon photonic technology, we believe that the aforementioned results on the dynamics of soliton propagation would be an interesting topic of research with potential applications in nonlinear plasmonics.

It would be particularly relevant to investigate the existence and stability properties of vectors solitons in non-Kerr media beyond the slowly varying envelope approximation. Noting that in many optical materials, the nonlinear refractive index deviates from the Kerr behavior for larger light intensities. In such media, an additional quintic nonlinearity arises due to fifth-order susceptibility [46]. Note that a self-defocusing fifth-order susceptibility $\chi^{(5)}$ usually accounts for the saturation of the third-order susceptibility $\chi^{(3)}$ [47]. Well known optical materials demonstrating nonideality of the nonlinear optical response include for example semiconductor waveguides (e.g., $Al_xGa_{1-x}As$, CdS, and $CdS_{1-x}Se_x$) and semiconductor-doped glasses (see, e.g., [48]). Considering the vectorial case, the dynamics of femtosecond optical pulse propagation in such systems should be described by the coupled

non-paraxial (2+1) dimensional nonlinear Schrödinger equation with cubic-quintic nonlinearity which represent the quintic generalization of the coupled cubic NLS equations. We note that finding the soliton pairs for such a problem may be a complicated task. Such interesting studies are in the scope of our future work and will be published elsewhere.

Acknowledgments

The authors thanks agencies DST, CSIR, NBHM, IFCPAR and DST-FCT, funded by the Government of India, for the financial support through major projects. KN acknowledgs CNRS for post doctoral fellowship at the Universite de Bourgogne, Dijon, and Agence Nationale de la Recherche (ANR) for the research fellowship at Universite de Grenoble-Alpes, Grenoble, France. We are also grateful to Dr. Fabio Biancalana for useful insight and fruitful discussions on soliton solution.

References

[1] J. M. Christian, G. S. McDonald, and P. Chamorro Posada, Journ. of Phys. A 40, 1545 (2007).

[2] M. Trippenbacha, W. Wasilewski a,P. Kruka, G.W. Bryantb, G. Fibichc, Y.B. Band, Opt. Commun. 210, 385391, (2002)

[3] M. Lax, W. H. Louisell, andW. B. McKnight, Phys. Rev. A 11, 1365 (1975)

[4] A. Ciattoni, B. Crosignani, P. D. Porto, J. Scheuer, and A. Yariv, Opt. Express 14, 5517 (2006); A. Ciattoni, B. Crosignani, S. Mookherjea, and A. Yariv, Opt. Lett. 5, 516 (2005); P. Chamorro-posada, G. S. McDonald, and G. H. C. New Journ. of Mod. Opt. 45, 1111 (1998); S. Chavez-Cerda and J. M. Hickmann, in Intern Quant. Electr. Conf., 2005. (2005), pp. 1798-1800.

[5] P. Chamorro-Posada, J. Sanchez-Curto, V. E. Grikurov, G. S. McDonald, and J. M. Christian, in 2008 Proceedings of the International Conference Days on Diffraction (2008), pp. 28-33; J. M. Christian, G. S. McDonald, and P. Chamorro-Posada, Journ. of Phys. Al 40, 1545 (2007); P. Chamorro-Posada and G. S. McDonald, Opt. Lett. 28, 825 (2003); J.

M. Christian, E. A. McCoy, G. S. McDonald, J. Snchez-Curto, and P. Chamorro-Posada, Journ. of Atom., Molec., and Opt. Phys. 2012, 21 (2012).

[6] S. Blair, Chaos 10, 570 (2000).

[7] K. Malakuti and E. Parilov, Appl. Num. Math. 61, 891 (2011).

[8] D. D. E. Temgoua and T. C. Kofane, Phys. Rev. E 91, 063201 (2015).

[9] P. C. Posada, G. S. McDonald, and G. H. C. New, in Technical Digest. Summaries of Papers Presented at the International Quantum Electronics Conference. Conference Edition. 1998 Technical Digest Series, Vol.7 (IEEE Cat. No.98CH36236) (1998), pp. 177-178.

[10] P. L. Chu, B. A. Malomed, and G. D. Peng, J. Opt. Soc. Am. B 10, 1379 (1993); L. F. Mollenauer and J. P. Gordon, eds., Chapter 1 - The Nonlinear Schrdinger Equation and Ordinary Solitons (Academic Press, Burlington, 2006), pp. 1 - 22.

[11] Y. S. Kivshar, IEEE Journl of Quant. Electr. 29, 250 (1993);

[12] B. B. Baizakov, S. M. Al-Marzoug, and H. Bahlouli, Phys. Rev. A 92, 033605 (2015); K. E. Strecker, G. B. Partridge, A. G. Truscott, and R. G. Hulet, New Journ. of Phys. 5, 73 (2003).

[13] K. Yuji, in Nonlinear Water Waves, edited by K. Horikawa and H. Maruo (Springer Berlin Heidelberg, Berlin, Heidelberg, 1988), pp. 85-91 ; A. Costa, A. R. Osborne, D. T. Resio, S. Alessio, E. Chrivvì, E. Saggese, K. Bellomo, and C. E. Long, Phys. Rev. Lett. 113, 108501 (2014).

[14] I. S. Kuwayama, Hidekazu, Scientifc Reports 3 (2013).

[15] A. I. Maimistov, Quant. Electr. 40, 756 (2010).

[16] C. Z. yun, H. N. ning, and X. Yi, Commun. in Theor. Phys. 12, 327 (1989).

[17] K. Sawada and T. Kotera, Prog. of Theor. Phy. 51, 1355 (1974).

[18] D. S. Wang, Comp. and Math. with Applic. 58, 146 (2009).

[19] G. Zhou and X. Bi, Wuhan Unive. Journ. of Nat. Sci. 14, 505 (2009).

[20] B. Tian and Y. T. Gao, Appl. Math. Lett. 10, 125 (1997).

[21] A. M. Wazwaz, Appl. Mathe. and Comp. 184, 1002 (2007).

[22] S. Bibi and S. T. Mohyud-Din, Journ. of the Assoc. of Arab Uni. for Basic and Appl. Sci. 15, 90 (2014).

[23] Q. M. Al-Mdallal and M. I. Syam, Chaos, Solitons and Fractals 33, 1610 (2007).

[24] X. Zhao and D. Tang, Phys. Lett. A 297, 59 (2002).

[25] M. Eslami, B. F. vajargah, and M. Mirzazadeh, Ain Shams Eng. Journ. 5, 221 (2014).

[26] A. Yildrim and Z. Pnar, Comp. and Mathe. with Applic. 60, 1873 (2010).

[27] Y. Yildrim and E. Yaar, Chin. Phys. B 26, 070201 (2017).

[28] G. Ebadi and A. Biswas, Comm. in Nonlin. Sci. and Number. Simu. 16, 2377 (2011).

[29] G. Ebadi and A. Biswas, Mathem. and Comp. Mod. 53, 694 (2011).

[30] Y. Gurefe and E. Misirli, AIP Conf. Procee. 1558, 1931 (2013).

[31] A. Biswas, M. Mirzazadeh, M. Eslami, Q. Zhou, A. Bhrawy, and M. Belic, Optik 127, 7250 (2016).

[32] H. Triki and A. M. Wazwaz, Phys. Let. A 380, 1260 (2016).

[33] H. Triki and A. M. Wazwaz, Waves in Rand. and Compl. Med. 27, 153 (2017).

[34] M. Mirzazadeh, Nonlin. Dyn. 82, 1775 (2015).

[35] LIU Cheng-Shi, Commun. Theor. Phys. (Beijing, China) 45, 395397, (2006)

[36] G. Agrawal, Nonlinear Fiber Optics (Academic Press, 2013); A. Hasegawa, Opt. Lett. 9, 288 (1984).

[37] P. J. Everitt, M. A. Sooriyabandara, M. Guasoni, P. B. Wigley, C. H. Wei, G. D. McDonald, K. S. Hardman, P. Manju, J. D. Close, C. C. N. Kuhn, et al., Phys. Rev. A 96, 041601 (2017); I. A. Bhat, T. Mithun, B. A. Malomed, and K. Porsezian, Phys. Rev. A 92, 063606 (2015).

[38] B. Ghosh and K. P. Das, Plasma Phys. and Contr. Fusion 27, 969 (1985); O. Bouzit, M. Tribeche, and A. S. Bains, Physics of Plasmas 22, 084506 (2015); N. Chowdhury, A. Mannan, M. Hossen, and A. Mamun Contrib. to Plasma Physics (2018).

[39] J. Beeckman, X. Hutsebaut, M. Haelterman, and K. Neyts, Opt. Express 15, 11185 (2007); T. P. Horikis, Phys. Lett. A 380, 3473 (2016); M. Peccianti, C. Conti, G. Assanto, A. D. Luca, and C. Umeton, Nature 432, 733 (2004).

[40] R. E. Noskov, P. A. Belov, and Y. S. Kivshar, Phys. Rev. Lett. 108, 093901 (2012); D. A. Korobko, S. G. Moiseev, and I. O. Zolotovskii, Opt. Lett. 40, 4619 (2015); M. Kumar, K. Porsezian, P. Tchofo-Dinda, P. Grelu, T. Mithun, and T. Uthayakumar, J. Opt. Soc. Am. B 34, 198 (2017); M. Kumar, K. Nithyanandan, and K. Porsezian, Phys.Rev. E 97, 062208 (2018).

[41] M. Brunetti and J. Kasparian, Phys. Let. A 378, 3626 (2014); C. N. Lashmore-Davies, D. R. McCarthy, and A. Thyagaraja, Physics of Plasmas 8, 5121 (2001); S. Kundu, S. Debsarma, and K. P. Das, Physics of Fluids 25, 066605 (2013).

[42] D. Salerno, P. D. Trapani, S. Minardi, S. Jenkins, T. A. B. Kennedy, G. Valiulis, and G. Tamosauskas, in EQEC '05. European Quantum Electronics Conference, 2005. (2005), p. 42; K. Staliunas, in 2013 Conference on Lasers ElectroOptics Europe International Quantum Electronics Conference CLEO EUROPE/IQEC (2013), pp. 1-1.; A. K. Mishra and A. Kumar, Journ. of Mod. Opt. 59,1599 (2012).; S. Kumar, R. Herrero, M. Botey, and K. Staliunas, Sci.Reports 5, 13268 (2015); V. K. Sharma, A. Goyal, T. S. Raju, C. Kumar, and P. K. Panigrahi, Opt. Fiber Techn. 24, 119 (2015); P. Béjot, B. Kibler, E. Hertz, B. Lavorel, and O. Faucher,Phys. Rev. A 83, 013830 (2011).

[43] H. Wang and W. She, Opt. Commun. 254, 145 (2005); M. Feng, Y. Xue,

Q. Wei, and J. L. Shi, Journ. of Shanghai Univ. (English Edition) 8, 159 (2004);

[44] F. Biancalana and C. Creatore, Opt. Express 16, 14882 (2008).

[45] K. Tamilselvan, T. Kanna, and A. Khare, Communications in Nonlinear Science and Numerical Simulation 39, 134 (2016).

[46] Z. Jovanoski and D. R. Roland, J. Mod. Opt. 48, 1179 (2001); S. Gatz and J. Herrmann, Opt. Lett. **17**, 484 (1992); H. Yanay, L.Khaykovich, and B. A. Malomed, Chaos 19, 033145 (2009).

[47] K. Nithyanandan, R. V. J. Raja, and K. Porsezian, Phys. Rev. A 87, 043805 (2013); Mohamadou, Alidou and LatchioTiofack, C. G. and Kofané, Timoléon C. Phy. Rev. E 82, 016601 (2010)

[48] P. Roussignol, D. Ricard, J. Lukasik, and C. Flytzanis, J. Opt. Soc. Am. B 4, 5 (1987); L.H. Acioli, A.S.L. Gomes, J.M. Hickmann, and C.B. de Araujo, Appl. Phys. Lett. 56, 2279 (1990); F. Lederer and W. Biehlig, Electron. Lett. 30, 1871 (1994).

[49] Q. Zhou, Poc. of the Rom. Aca., 18, 223,2017; A. Biswas, M. Mirzazadeh, M. Eslami, Q. Zhou, A. Bhrawj, M. Belic, Optik, 145, 650, (2017); N. Taghizadeh, Q. Zhou, M. Ekici, M. Mirzazadeh, Superlatt. and Microstruct., 102, 323(2017); A. Biswas, M. Ekici, A. Sonmezoglu,Q. zhou, A. S. Alshomrani, S. P. Moshokoa, M. Belic; Eur. Phys. J. Plus, 133, 204 (2018).

[50] W. Yu, Q. Zhou, M. Mirzazadeh, W. Liu, A. Biswas, Journ. of Adv. Res. 15, 69,(2019); Y. Zhang, C. Yang, W. Yu, M. Mirzazadeh, Q. Zhou, W. Liu; Nonlin. Dyn. 94, 1351 (2018); X. Liu, H. Triki, Q. Zhou, M. Mirzazadeh, W. Liu, A. Biswas, M. Belic, Nonlin. Dyn, 95, 143 (2019); C. Yang, W. Liu, Q. Zhou, D. Mihalache, B. A. Malomed, Nonlin. Dynam. 95, 369 (2019)

[51] A. Biswas, Y.Yildirim, E. yasar, H. Triki, A. S. Alshomrani, M. Z. Ullah, Q. Zhou, S. P. Moshokoa, Optik, 158, 399, (2018); A. Biswas, Y. Yildrim, E. Yasar, Q. Zhou, S. P. Moshokoa, M. Belic, Optik, 160, 24, (2018)

[52] A. Sonmezoglu, M. Yao, M. Ekici, M. Mirzazadeh, Q. Zhou, Nonlin. Dynam., 88, 595, (2017)

[53] M. Ekici, M. Mirzazadeh, A. Sonmezoglu, Q. Zhou, H. Triki, M. Z. Ullah, S. P. Moshokoa, A. Biswas, Optik, 131, 964, (2017)

[54] A. Biswas, A. H. Kara, M. Z. Ullah, Q. Zhou, H. Triki, M. Belic, Optik (2017), 145, 650 (2017)